

Contract No:

This document was prepared in conjunction with work accomplished under Contract No. DE-AC09-08SR22470 with the U.S. Department of Energy (DOE) Office of Environmental Management (EM).

Disclaimer:

This work was prepared under an agreement with and funded by the U.S. Government. Neither the U. S. Government or its employees, nor any of its contractors, subcontractors or their employees, makes any express or implied:

- 1) warranty or assumes any legal liability for the accuracy, completeness, or for the use or results of such use of any information, product, or process disclosed; or
- 2) representation that such use or results of such use would not infringe privately owned rights; or
- 3) endorsement or recommendation of any specifically identified commercial product, process, or service.

Any views and opinions of authors expressed in this work do not necessarily state or reflect those of the United States Government, or its contractors, or subcontractors.

Inhibition of Pitting Corrosion in Simulated Liquid Radioactive Waste

R. E. Fuentes and B. J. Wiersma
Savannah River National Laboratory
SRS Road 1A
Aiken, SC, 29808
USA

K. D. Boomer and A. J. Feero
Washington River Protections Services
2440 Stevens Rd.
Richland, WA
USA

ABSTRACT

The Hanford Site in Richland, WA stores liquid radioactive waste in underground, carbon steel tanks. The tanks have a well-defined chemistry control program for the prevention of stress corrosion cracking, general corrosion and pitting of the steel that is exposed to the waste. The primary aggressive species active in the localized mechanism is nitrate, while hydroxide and nitrite are utilized to inhibit these mechanisms. Recent tests suggested that the corrosion control program requirements may be optimized so that the total amount of inhibitor necessary may be reduced. Secondly, future waste streams that will be transferred into the tanks may include other aggressive species (e.g., chloride and sulfate) at higher than previously experienced concentrations. Electrochemical corrosion testing was performed to determine new limits that optimize the chemistry control, yet are robust enough to inhibit against the possibility of increased concentrations of aggressive species.

Key words: radioactive waste, carbon steel, pitting corrosion, electrochemical testing

INTRODUCTION

Weapons, space and medical research programs led by the U. S. Department of Energy have created a legacy of nuclear waste over the past 70 years. At the Hanford site in Richland, WA, the liquid waste is being stored on an interim basis in 149 single shell tanks (SST) and 28 double shell tanks (DST) (see Figure 1). The final disposition of the liquid waste into a solid form, either vitrified glass or a grout formulation, will likely take several more decades. Understanding potential degradation mechanisms

are a key to preserving the structural and leak integrity of the waste tanks, particularly the DSTs, until final disposition of the waste. Presently, the site implements a corrosion control program to maintain the waste chemistry while the waste is being stored within requirements that mitigate corrosion mechanisms such as stress corrosion cracking, pitting and general corrosion.

In preparation for starting the vitrification facility, waste is being retrieved from the SSTs and transferred to the DSTs. Additionally, with the eventual start-up of the vitrification facility, streams of waste may be returned to the DSTs. The tank farm facility is reviewing and evaluating material balance projections to determine the impact of these processes on the waste chemistry. Initial projections suggest that the waste chemistry of the DSTs may shift to a broader range of pH and higher aggressive anion concentrations (e.g., chloride, sulfate, etc.) than the wastes that are presently stored. Therefore, in conjunction with this evaluation, the corrosion control program is being assessed to ensure that it is robust and can adjust to these anticipated changes.

The present corrosion control program mitigates corrosion of carbon steel due to the nitrate ion by addition of sodium hydroxide to the tanks to raise the pH of the waste and reliance upon radiolysis to deplete the nitrate ion to the nitrite ion, which inhibits corrosion. The inhibitor requirements for are exhibited in Table 1. These limits were developed based on laboratory testing that evaluated specific corrosion mechanisms. For nitrate concentrations greater than 1 M, stress corrosion cracking and general corrosion are mitigated, while for nitrate concentrations less than 1 M pitting and general corrosion are mitigated. Presently, the supernate concentrations in the DSTs are well above 1 M hydroxide, which will mitigate all three mechanisms. However, the process changes mentioned above, and the potential for hydroxide depletion within the interstitial liquid of the waste solids, may challenge these requirements in the future.

Testing has been performed previously to address apparent gaps in the sections of the corrosion control program that address stress corrosion cracking¹. However, a similar program has not been performed to investigate pitting corrosion over the entire range of anticipated concentrations. This testing program specifically targets gap regions such as the pH range between 10 and 13.5 and will address chloride concentrations up to 0.4 M and sulfate concentrations up to 0.2 M and evaluates the likelihood of pitting corrosion. Optimization (i.e., managing the total inhibitor concentration added) of the inhibitor scheme such that the amount of sodium that needs to be added will also constrain the test matrix. This paper presents the test procedure, the statistical design and approach to analysis of initial test results.

EXPERIMENTAL PROCEDURE

Materials Tested

Carbon steel electrodes in the form of “bullets”, with dimensions 0.477 cm diameter and 3.17 cm long, were used for the testing. The coupons were fabricated from Association of American Railroads⁽¹⁾ Tank Car (AAR TC) 128 Steel. This steel was selected for testing since it approximates the chemistry and microstructure of UNS K02401 [i.e., American Society for Testing and Materials (ASTM)⁽²⁾ A515 Grade 60 carbon steel], the steel from which the tanks were fabricated. The AARTC 128 steel was also selected because it was of the same vintage as the tank steel. The chemical composition of the steel is shown in Table 2. The yield strength for the material was greater than 380 MPa and the ultimate tensile strength was greater than 550 MPa. All elemental compositions except for Mn and Si meet the ASTM specification. The Mn is greater than the maximum allowed of 0.9 wt.%, while the Si is less than

⁽¹⁾ American Association of Railroads, 425 3rd Street SW, Washington, DC 20024

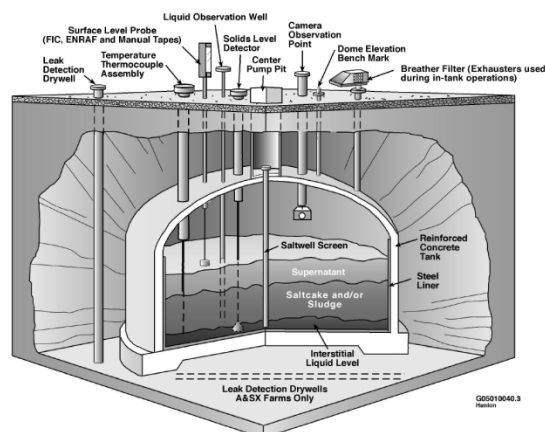
⁽²⁾ ASTM International, 100 Barr Harbor Dr., West Conshohocken, Pa 19428-2959

the required range. The higher Mn could explain the higher than specified tensile properties as well (e.g., ultimate strength between 410 MPa to 500 MPa required).

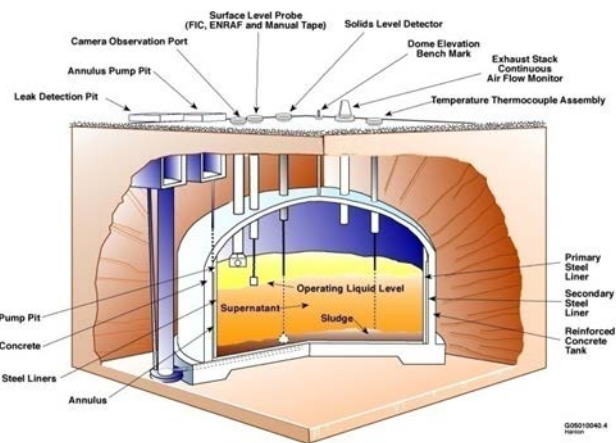
Table 1. Double-Shell Tank Waste Chemistry Limits for Corrosion Control.

For $[\text{NO}_3^-]$ Range	Variable	For Waste Temperature (T) Range		
		$T < 167\text{ }^\circ\text{F (75 }^\circ\text{C)}$	$167\text{ }^\circ\text{F (75 }^\circ\text{C)} \leq T \leq 212\text{ }^\circ\text{F (100 }^\circ\text{C)}$	$T > 212\text{ }^\circ\text{F (100 }^\circ\text{C)}$
$[\text{NO}_3^-] \leq 1.0\text{M}$	$[\text{OH}^-]$	$0.010\text{M} \leq [\text{OH}^-] \leq 8.0\text{M}$	$0.010\text{M} \leq [\text{OH}^-] \leq 5.0\text{M}$	$0.010\text{M} \leq [\text{OH}^-] \leq 4.0\text{M}$
	$[\text{NO}_2^-]$	$0.011\text{M} \leq [\text{NO}_2^-] \leq 5.5\text{M}$	$0.011\text{M} \leq [\text{NO}_2^-] \leq 5.5\text{M}$	$0.011\text{M} \leq [\text{NO}_2^-] \leq 5.5\text{M}$
	$[\text{NO}_3^-] / ([\text{OH}^-] + [\text{NO}_2^-])$	< 2.5	< 2.5	< 2.5
$1.0\text{M} < [\text{NO}_3^-] \leq 3.0\text{M}$	$[\text{OH}^-]$	$0.1 ([\text{NO}_3^-]) \leq [\text{OH}^-] < 10\text{M}$	$0.1 ([\text{NO}_3^-]) \leq [\text{OH}^-] < 10\text{M}$	$0.1 ([\text{NO}_3^-]) \leq [\text{OH}^-] < 4.0\text{M}$
	$[\text{OH}^-] + [\text{NO}_2^-]$	$\geq 0.4 ([\text{NO}_3^-])$	$\geq 0.4 ([\text{NO}_3^-])$	$\geq 0.4 ([\text{NO}_3^-])$
$[\text{NO}_3^-] > 3.0\text{M}$	$[\text{OH}^-]$	$0.3\text{M} \leq [\text{OH}^-] < 10\text{M}$	$0.3\text{M} \leq [\text{OH}^-] < 10\text{M}$	$0.3\text{M} \leq [\text{OH}^-] < 4.0\text{M}$
	$[\text{OH}^-] + [\text{NO}_2^-]$	$\geq 1.2\text{M}$	$\geq 1.2\text{M}$	$\geq 1.2\text{M}$
	$[\text{NO}_3^-]$	$\leq 5.5\text{M}$	$\leq 5.5\text{M}$	$\leq 5.5\text{M}$

Figure A-3. Single-Shell Tank Instrumentation Configuration



(a)



(b)

Figure 1. Drawings depicting Hanford waste tanks: (a) single shell tank (SST) and (b) double shell tank (DST)

**Table 2
Chemical Composition of AAR TC 128 Steel (wt.%)**

	C	Mn	P	S	Si	Fe
Specification	0.24 (max.)	0.9 (max.)	0.035 (max.)	0.04 (max.)	0.13 to 0.33	Balance
Measured	0.212	1.029	0.012	0.013	0.061	Balance

Figure 2 shows the microstructure of the rail car steel as exhibited in the longitudinal and transverse orientation. A banded, ferrite/pearlite matrix was observed. The transverse orientation also exhibited several inclusions, likely manganese sulfide inclusions. These could be sites for pit initiation².

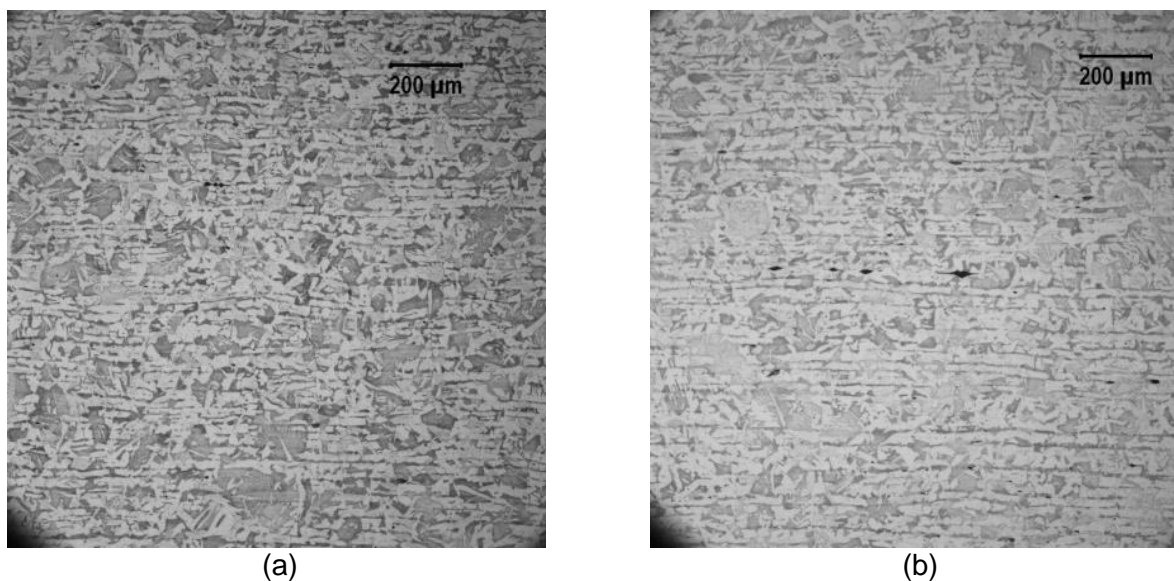


Figure 2: Microstructure of AAR TC Steel (a) longitudinal, (b) transverse.

Before testing, a drill was used to polish the sample to a 600-grit finish. The electrodes were examined with a stereomicroscope and in some cases visually for any defect and to ensure that the sample had a homogeneous surface. Then they were rinsed with distilled water and acetone. Figure 3 shows a picture of the sample after being polished and rinsed. It shows the surface of the shank and nose of the bullet. The bullet was attached to a stainless steel rod protected by a glass holder. A PTFE fixture was used to prevent liquid contact with the stainless steel rod and ensure electrical isolation.



Figure 3: Side picture of the carbon steel in "bullet" electrode.

Solutions Tested

Reagent grade chemicals were used to prepare the simulants. The tests were conducted at temperatures 25, 35 and 50 °C and pH of approximately 10.0 and 13.3. Table 3 shows the chemical species and the chemical used to simulate the concentration. Total Inorganic Carbon (TIC)

concentration was maintained at 0.1 M and depending of pH requirements was adjusted by using sodium bicarbonate.

Test Apparatus and Set-up

A potentiostat was utilized in this study to perform the electrochemical testing. Prior to use, the ASTM G5³ standard was performed with the potentiostat for quality assurance. ASTM G5 protocols were also run at the end of testing. Approximately 700 mL of simulant was added to the cell to cover the working electrode (i.e. carbon steel “bullet”). Two carbon graphite rods served as the counter electrode. A saturated calomel electrode (SCE) was used as the reference electrode. The SCE was placed in a bridge containing 0.1 NaNO₃ solution. The cell was placed on top of a hotplate with temperature control. The tests were performed at quiescent, aerated conditions. The testing consisted of monitoring the open circuit potential (OCP) for two hours to ensure equilibration of the carbon steel in solution. Then, a cyclic potentiodynamic polarization (CPP) test was conducted by applying a cyclic potential ramp from -50 mV vs. OCP up to a vertex threshold current of 1 mA/cm² at a scan rate of 0.167 mV/s. The potential was returned back to the OCP to complete the test. Duplicate tests were run for each solution condition.

Table 3. Chemical used to simulate chemical species found.

Chemical component	Chemical used
Hydroxide	Sodium Hydroxide
Nitrite	Sodium Nitrite
Nitrate	Sodium Nitrate
Chloride	Sodium Chloride
Sulfate	Sodium Sulfate
TIC	Sodium carbonate
	Sodium bicarbonate

Negative hysteresis in the CPP scan, where the reverse scan current density is less than the forward scan current density, was considered to be a condition where there was no pitting susceptibility. Positive hysteresis, where the reverse scan current density is greater than forward scan current density, on the other hand was considered to be a condition where there was pitting susceptibility. The result was confirmed by examination of the sample for pitting. In some cases, the difference between the repassivation potential and the zero current potential is positive and relatively large (e.g., greater than 200 mV). In this case, the condition was considered to be a pass, even though pits may initiate, insignificant growth is anticipated.

STATISTICAL DESIGN AND ANALYSIS OF TESTS

A Plackett-Burman statistical design was used to identify the major variables affecting pitting corrosion⁴. This design is utilized to screen the variable space in selected portions of a 2ⁿ factorial design where one variable is changed at a time with a maximum and minimum value for each independent variable. As a screening design, the Plackett-Burman test series has the advantage that a relatively small number of experiments was required to investigate a large number of independent variables. On the

other hand, the design eliminates interaction effects, such as the effects of inhibitors, and presents them as an inflation of experimental error.

Because many independent variables can affect pitting, the Plackett-Burman test series included six independent variables, five anion concentrations and temperature as shown in Table 4. Conditions that were held constant for the testing, carbonate concentration, are also shown in the table. The repassivation potential minus zero current potential for the CPP test ($E_{rp} - E_{zc}$) was selected as the dependent variable, which is a measure of the susceptibility a material to pitting corrosion in a given environment⁵. This approach required 15 experiments rather than 128 for a 2^n factorial matrix with one maximum and one minimum value for each independent variable. The design efficiency achieved was very good at approximately 80% (predictions are 80% as precise as the most precise experimental design possible).

Once these tests were completed, a Box-Behnkin statistically designed matrix was developed to explore the interaction effects⁶. Tests were recommended at appropriate combinations of the minimum, mean and maximum values for the independent variables. This statistical series also effectively reduces quantity of tests that need to be performed as compared to a full factorial design. The results may be analyzed to evaluate interaction terms between the variables.

A multiple regression, least squares analysis was utilized to model the dependent variable, $E_{rp} - E_{zc}$, as a function of the dependent variables. The Plackett-Burman provided a linear equation, while the Box-Behnkin series will provide a model with cross-product and squared terms.

Table 4. Variables and Constants for Anticipated Stream Conditions for Plackett-Burman Test Series

Independent Variables		
	Minimum	Maximum
Hydroxide (M)	0.0001	0.6
Nitrite (M)	0.0	1.2
Nitrate (M)	0.0	5.5
Chloride (M)	0.0	0.4
Sulfate (M)	0.0	0.2
TIC (M)	0.1	
Temperature	20	50

RESULTS

Plackett-Burman statistical series produced fifteen experiments shown in Table 5. Twelve of those experiments reflect the maximum and minimum value for the independent variables while maintaining the carbonate at 0.1 M. One experiment indicates the middle value for the independent variables and is being performed in triplicate for statistical significance. This experiment corresponds to test 8, 11 and 14 and is gray shaded in the table.

Table 5 Plackett-Burman Statistical Design Simulant Compositions

Independent Variable	Test														
	1	2	3	4	5	6	7	8	9	10	11	12	13	14	15
Hydroxide	0.6	0.6	0.6	0.6	0.0001	0.0001	0.6	0.3	0.0001	0.6	0.3	0.0001	0.0001	0.3	0.0001

[OH]															
Nitrite [NO ₂]	1.2	1.2	1.2	0	0	0	0	0.6	1.2	0	0.6	0	1.2	0.6	1.2
Nitrate [NO ₃]	5.5	5.5	0	5.5	5.5	5.5	0	2.75	0	0	2.75	0	0	2.75	5.5
Chloride [Cl]	0.4	0	0	0.4	0	0	0	0.2	0	0.4	0.2	0.4	0.4	0.2	0.4
Sulfate [SO ₄]	0.2	0	0	0.2	0.2	0	0.2	0.1	0.2	0	0.1	0	0.2	0.1	0
TIC	0.1	0.1	0.1	0.1	0.1	0.1	0.1	0.1	0.1	0.1	0.1	0.1	0.1	0.1	0.1
Temperature (°C)	50	50	20	20	50	20	20	35	50	50	35	50	20	35	20

Electrochemical testing was performed and Figs. 3 to 5 show an example of a typical CPP scan obtained for some of the tests for the sample and duplicate. The zero current potential is also illustrated in this figure. At the right side of the figure there are two pictures corresponding to the nose and shank of the carbon steel “bullet”. These pictures were taken on a microscope to identify localized corrosion on the samples after test.

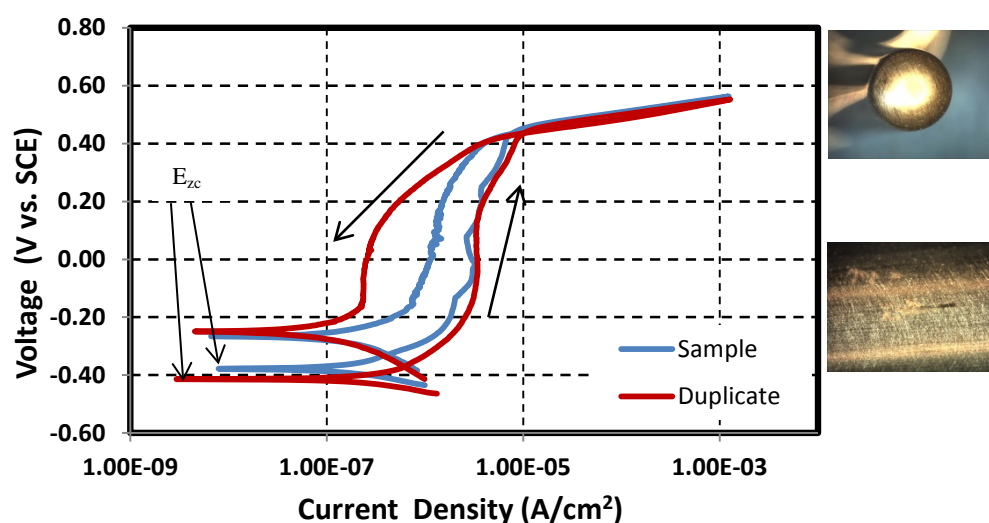


Figure 3: Cyclic potentiodynamic polarization scans and pictures for sample and duplicate using conditions described in Test 2

As observed in the CPP diagram in Figure 3, the scan starts a sweep to high potentials until it reaches the transpassive region. Then it returns at lower current densities than the forward scan indicating negative hysteresis. The negative hysteresis was obtained for Tests 2, 3, 7, 9 and 10. As seen in the pictures, negative hysteresis induces in most cases no pits on the sample. For these cases, the repassivation potential is taken at the point where it intersects the passive current density for the forward scan. The results observed in Figure 3 are the opposite of what is observed in the CPP scan in Figure 4. For this scan, low current densities are seen at the forward scan and continue to higher current densities for the reverse scan. This indicates a positive hysteresis and was obtained for Tests 4, 5, 6, 8, 11, 12 and 14. Figure 4 shows the particular CPP results for test 5. For this occurrence the repassivation potential minus the zero current potential is taken as 0.

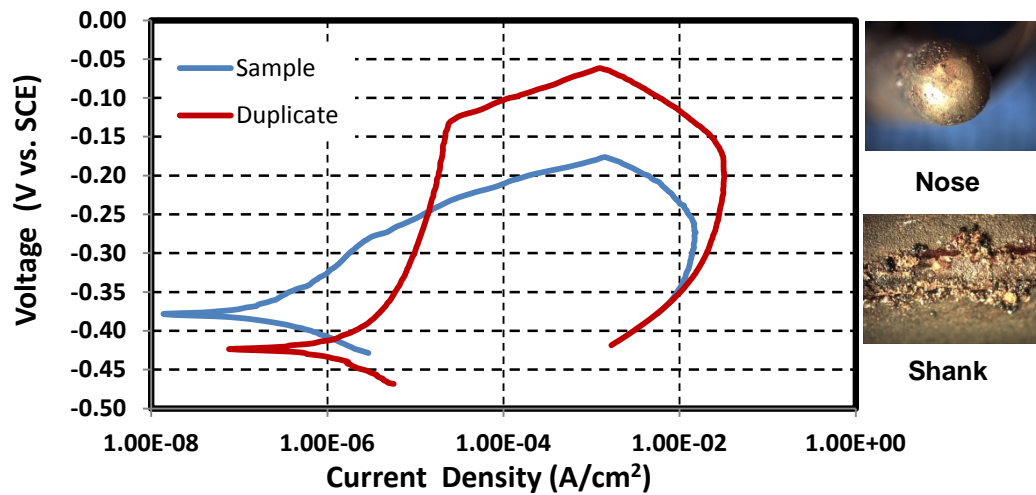


Figure 4: Cyclic potentiodynamic polarization scans and pictures for sample and duplicate using conditions described in Test 5

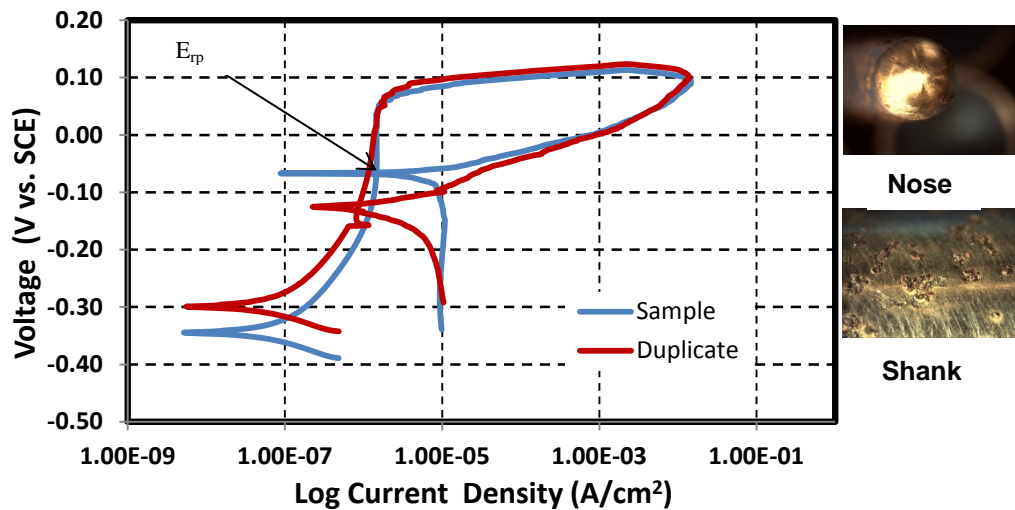


Figure 5: Cyclic potentiodynamic polarization scans and pictures for sample and duplicate using conditions described in Test 15

Other CPP scan behavior obtained can be seen in Figure 5. For this case positive hysteresis is also observed. However, before the potential has returned to E_{zc} the current density decreases to values below the forward scan passive current density. The intersection between the reverse scan current density and the forward scan passive current density corresponds to the repassivation potential (E_{rp}). This behavior was observed for Tests 1, 13, and 15. Table 6 shows a summary of the entire testing with the results of the dependent variable chosen: $E_{rp}-E_{zc}$ and if pitting was observed for the condition and its duplicate.

Table 6 Results from CPP tests

Test	Hysteresis		$E_{rp}-E_{zc}$		Pitting on Sample?	
	Sample	Duplicate	Sample	Duplicate	Sample	Duplicate
1	Positive	Positive	332	70	Major	Major
2	Negative	Negative	818	850	No	No
3	Negative	Negative	883	870	No	No
4	Positive	Positive	0	0	Major	Major
5	Positive	Positive	0	0	Major	Major
6	Positive	Positive	0	0	Major	Major
7	Negative	Negative	850	867	No	No
8	Positive	Positive	0	0	Minor	Major
9	Negative	Negative	952	923	No	No
10	Negative	Negative	808	816	Minor	No
11	Positive	Positive	0	0	Minor	Minor
12	Positive	Positive	0	0	Major	Major
13	Positive	Positive	280	245	Major	Major
14	Positive	Positive	0	0	Minor	Minor
15	Positive	Positive	406	173	Major	Major

A multiple regression, least squared analysis was used to develop a linear model fit for the dependent variable $E_{rp} - E_{zc}$. Equation 1 shows the linear model and the coefficients are shown Table 7. As expected, the coefficients for the inhibitor species are positive, while the coefficients for the aggressive species are negative. The significance of the variable, as determined by the T statistic, is also shown in Table 7. The T statistic is used to conduct hypothesis tests on regression coefficients obtained in simple linear regression. A statistic based on the t distribution is used to test the two-sided hypothesis that the true slope, B1 equals a constant value, B10. Coefficients with T values less than 0.05 are considered statistically significant.

$$E_{rp} - E_{zc} (V) = A + B[Nitrite] + C [Chloride] + D [Nitrate] + E [Sulfate] + F[Hydroxide] + G [Temperature]$$

(1)

Table 7. Coefficients for Equation 1 fit to the Plackett-Burman test matrix results.

Species	Coefficient (mV)	T Statistic
Intercept	338	0.0434
Nitrite (M)	177	0.0391
Chloride (M)	-619	0.0179
Nitrate (M)	-60	0.0026
Hydroxide (M)	757	0.0002
Sulfate (M)	-838	0.098
Temperature (°C)	0.24	0.9411

The statistical analysis indicated that the linear coefficients for nitrite, chloride, nitrate and hydroxide were significant. The sulfate coefficient is large and does indicate some degree of significance and thus this variable will continue to be explored in future tests. Temperature on the other hand showed practically no influence on the model equation over the given range. This result was unexpected as corrosion typically shows a strong dependence on temperature⁷. Although future statistical designs may initially discount the effect of temperature in this range, the effect of this typically significant variable will be re-visited with future tests.

The Plackett-Burman model provides an indication of the significant terms for modeling the dependent variable response, however, it does not provide information on the interaction between the inhibitor and aggressive species (i.e., cross product terms, etc.). To establish these interaction terms, these a Box-Behnkin test matrix was developed as shown in Table 8. This test matrix contains not only maximum and minimum values, but mid-point values within the test ranges. These tests will be performed at a temperature of 35 °C, which is the mid-point of the temperature range. Completion of these tests will increase confidence in the model equation and allow the establishment of corrosion control limits.

SUMMARY AND CONCLUSIONS

Cyclic potentiodynamic polarization is being utilized to explore the effects of various anions and temperature on pitting corrosion in simulated radioactive waste solutions. Statistically designed tests are being utilized to determine the significance and interaction between these variables. A Plackett-Burman test series determined that nitrate, nitrite, chloride, sulfate and hydroxide were statistically significant, while temperature was not significant within the variable test ranges. A linear multiple regression, least squared model was proposed to predict pitting susceptibility as measured by the dependent variable $E_{rp} - E_{zc}$. Further testing will be performed with a Box-Behnkin test series to establish interaction terms between the variables.

ACKNOWLEDGEMENTS

The authors gratefully acknowledge the assistance of Kevin Kalbaugh in the set-up and performance of the tests. The assistance of Dr. Stephen Harris, was essential for the development of the statistical test designs and analysis.

REFERENCES

1. L. M. Stock, J. R. Follett, and E. C. Shallman, "Specifications for the Minimization of the Stress Corrosion Cracking Threat in Double-Shell Tank Wastes," RPP-RPT-47337, Washington River Protection Solutions, Richland, WA, March 2011.
2. Z. Szlarska-Smialowska, Corrosion, Vol. 28, p. 388, 1972.
3. ASTM Standard G5, "Standard Reference Test Method for Making Potentiostatic and Potentiodynamic Measurements", Annual book of ASTM Standards, Philadelphia, PA.
4. R. L. Plackett and J. P. Burman, Biometrika, Vol. 33, p. 305, 1946.
5. D. C. Silverman, Corrosion 98, Paper No. 299, NACE International, Houston, TX, 1998.
6. G. E. P. Box and D. W. Behnkin, Technometrics, Vol. 2, p. 455, 1960.
7. P. E. Zapp and D. T. Hobbs, Corrosion 92, Paper No. 98, NACE International, Houston, TX, 1992.

Table 8. Box-Benhkin Statistical Design

Test	Hydroxide (M)	Nitrite (M)	Nitrate (M)	Chloride (M)	Sulfate (M)
1	0.6	1.2	5.5	0.4	0.2
2	0.6	1.2	5.5	0	0
3	0.6	1.2	0	0	0
4	0.6	0	5.5	0.4	0.2
5	0	0	5.5	0	0.2
6	0	0	5.5	0	0
7	0.6	0	0	0	0.2
8	0.3	0.6	2.75	0.2	0.1
9	0.3	0.6	2.75	0.2	0.1
10	0.6	1.2	0	0	0.2
11	0.6	0	0	0.4	0
12	0.3	0.6	2.75	0.2	0.1
13	0.3	0.6	2.75	0.2	0.1
14	0	0	0	0	0.1
15	0	1.2	0	0	0.2
16	0.3	0.6	2.75	0.2	0.1
17	0.3	0.6	2.75	0.2	0.1
18	0	1.2	5.5	0.4	0
19	0.3	0	0	0.2	0.2
20	0.6	0	5.5	0.4	0
21	0.6	1.2	2.75	0.2	0.1
22	0.3	0	0	0	0

23	0.3	0.6	5.5	0.2	0.1
24	0.6	0.6	2.75	0.2	0
25	0.3	1.2	5.5	0	0.1
26	0.3	0.6	2.75	0	0.2
27	0	0.6	0	0.2	0
28	0	1.2	5.5	0.2	0.2
29	0	1.2	2.75	0	0
30	0.6	0	2.75	0	0.1
31	0	0.6	0	0	0.1
32	0.3	0	5.5	0.2	0.1
33	0.6	0.6	5.5	0	0.2
34	0.3	1.2	0	0.4	0
35	0.6	0.6	0	0.4	0.1
36	0	0	2.75	0.4	0.1
37	0.3	0.6	2.75	0.4	0.2
38	0	0.6	5.5	0.4	0.2